

Characteristics of a thermal neutrons scintillation detector with the $[\text{ZnS}(\text{Ag})+{}^6\text{LiF}]$ at different conditions of measurements

V.V. Alekseenko^a, I.R. Barabanov^a, R.A. Eteзов^a, Yu.M. Gavrilyuk^a,
A.M. Gangapshev^a, A.M. Gezhaev^a, V.V. Kazalov^a, A.Kh. Khokonov^b,
V.V. Kuzminov^a, S.I. Panasenکو^c, S.S. Ratkevich^c

^a *Institute for Nuclear Research, RAS, Russia*

^b *Kh.M. Berbekov Kabardino-Balkarian State University, Russia*

^c *V.N. Karazin Kharkiv National University, Ukraine*

A construction of a thermal neutron testing detector with a thin $[\text{ZnS}(\text{Ag})+{}^6\text{LiF}]$ scintillator is described. Results of an investigation of sources of the detector pulse origin and the pulse features in a ground and underground conditions are presented. Measurements of the scintillator own background, registration efficiency and a neutron flux at different objects of the BNO INR RAS were performed. The results are compared with the ones measured by the ${}^3\text{He}$ proportional counter.

I. INTRODUCTION

Large area scintillation detector of the thermal neutrons on a base of a thin $[\text{ZnS}(\text{Ag})+{}^6\text{LiF}]$ scintillator has been put into operation at the Baksan Neutrino Observatory of the INR RAS at the last time [1, 2]. The neutron registration is occurred as a result of ${}^6\text{Li}(n, \alpha){}^3\text{H}+4786$ keV reaction. The cross section is 945 b [3]. A kinetic energy of the reaction products ($E_\alpha = 2051$ keV, $E_{\text{H}} = 2735$ keV) converted at a light flash by the scintillator. The scintillator components enter into the composition as an alloy. Spectrometric characteristics of such detectors are known not enough. The aim of the work was to investigate and refinement these parameters.

II. DETECTOR CONSTRUCTION

A schematic view of the test detector and its electronics are shown on the Fig. 1. The detector is assembled in a rectangular case with $30 \times 30 \times 50$ cm³ sizes made from galvanized iron of the 0.7 mm thickness. The covers of the top and bottom are detachable. A dividing plate with a central 150 mm diameter hole aimed to install photomultiplier FEU-173 (PMT) mounted in the middle of the case. A charge sensitive preamplifier (CSP) with ~ 100 μs self-discharge time is installed on the wall inside of the upper part of the case. Pulses from the PMTs anode resistor (4.8 M Ω) go to the CSP input and further at the input of the LAn-10M5 digital oscilloscope card and are recorded into the personal computer (PC) memory. A sampling frequency was equal to 6.25 MHz. The flat flexible plate with the $[\text{ZnS}(\text{Ag})+{}^6\text{LiF}]$ scintillator is placed on the floor of the bottom section. It contains of the white sheet of plastic film (207×295 mm²) with a sticky side covered by grains of the scintillator with an average thickness of ~ 0.1 mm [2]. The sheet is laminated by the lamsan films. A surface of the bottom section covered with a reflecting mylar film for a better light collection. Densities of the pure $\text{ZnS}(\text{Ag})$ and ${}^6\text{LiF}$ are equal to 4.09 g·cm⁻³ [4] and ~ 2.64 g·cm⁻³ [7]. A density

of the mixture in the proportion 1 : 3 is ~ 3 g·cm⁻³.

III. RESULTS OF MEASUREMENTS

The two types of working pulses shown on the Fig. 2 (*a, b*) were observed in a measurement with the detector at the ground laboratory. The first type (*a*) has a front time duration $\tau_f = 16 - 25$ μs which corresponds to the own de-excitation time of the fine-grained scintillator $\tau_s = 8 - 10$ μs ($\tau_f = 3\tau_s$). The CSP integrates an input current and a pulse maximum is shapes at the point where the current charging velocity turns equal to the preamplifier own charge decay velocity. The second type (*b*) of a pulse has a front time duration $\tau_f = 0.8\tau_s$. Its shape is similar to the noise pulses which occur after an irradiation of the scintillator and PMT by an external light during of an adjustment work. Intensity and amplitudes of the noise pulses in the range of interest are fall down to zero after some hours. A residual part of the type (*b*) pulses is not a noise because of its intensity is proportional to the intensity of cosmic rays and decreases with moving of the detector on a deeper underground. It is known that a part of a photomultiplier own noise pulses could be created by the charged particles from an outer radioactive background and cosmic rays and also by charged particles appeared in decays of radioactive residual impurity isotopes in the PMT construction materials [6]. A separate investigation was done for an alignment of a type (*b*) appearing mechanism. The two possibilities were examined. The first one is a direct generation of the primary electrons from the photocathode or dynode by the cosmic rays. The second one is an appearing of a photoelectron from the photocathode as a result of absorption of a Cerenkov radiation created by a charged particle in a glass of the entrance window of the PMT. For the last case, the cosmic rays coming from directions around the vertical can generate in the window a Cerenkov radiation directed outside. This light will return into the PMT after the reflection from the bottom sell walls. The PMT entrance window was cov-

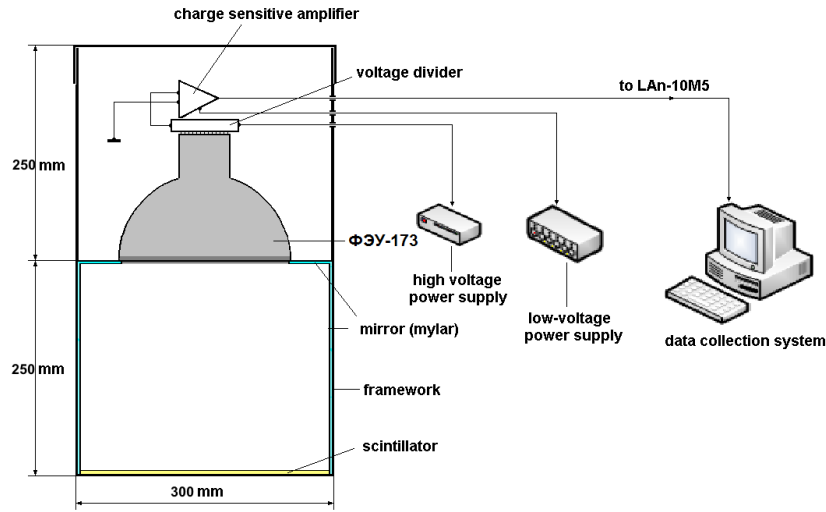


FIG. 1. A schematic view of the test detector with the $[\text{ZnS}(\text{Ag})+{}^6\text{LiF}]$ scintillator and its electronics.

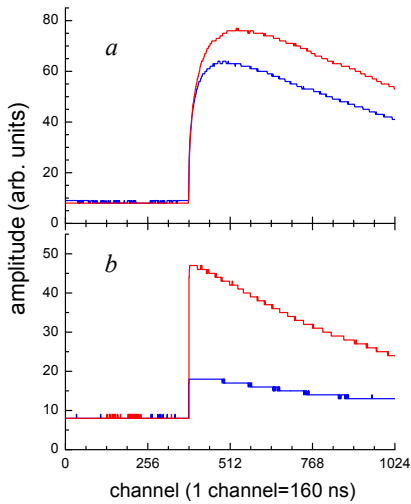


FIG. 2. The two types of pulses with test the detector. “a” - the long pulse rise time, “b” - the short pulse rise time.

ered by the black paper to check this assumption. The pulses with a short front only remained in the spectrum. Their intensity is changed with the cosmic rays intensity at a moving of the detector from the second floor of a laboratory building to the ground one. A conclusion that the short pulses are generated by cosmic rays in the photocathode or dynode has been made.

A set of measurements was made with the detector at the ground and underground conditions of the BNO INR RAS. They are:

1. Deep Underground Low Background Laboratory (DULB-4900). An unshielded place located at the underground hall under the mountain thickness equal to the 4900 m of the water equivalent (m w.e.). First spectrum (a) was measured without any shielding materials and the second one (b) was

measured with the $0.1 \times 100 \times 100 \text{ cm}^3$ Cd sheet (absorber) placed under the detector;

2. DULB-4900 low background compartment with the walls made of 25 cm polyethylene +0.1 cm Cd+15 cm Pb. A spectrum (a) was measured;
3. “2” + thermal neutron source;
4. Low background underground laboratory “KAPRIZ” at the 1000 m w.e. The spectra (a) and (b) were measured;
5. Low background underground laboratory “NIKA” at the 660 m w.e. The spectra (a) and (b) were measured;
6. Underground hall of the “CARPET-2” set-up muon detector at the 5 m w.e. The spectra (a) and (b) were measured;
7. Ground building “ELLING” of the “CARPET-2” set-up. The spectra (a) and (b) were measured;
8. The open soil. The spectra (a) and (b) were measured;
9. The fourth floor (room 404) of the four-storey laboratory building (LAB). The spectrum (a) was measured;
10. The river side of the second floor (room 204) of the four-storey laboratory building. The spectra (a) and (b) were measured;
11. The valley side of the second floor (room 211) of the four-storey laboratory building. The spectrum (a) was measured;
12. The ground floor of the four-storey laboratory building. The spectrum (a) was measured.

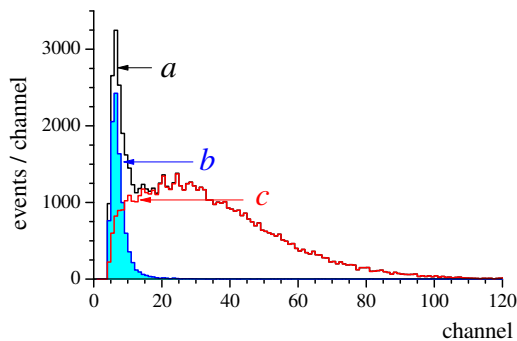


FIG. 3. Pulse amplitude spectra of the detector in the point (10) collected at 63.12 h: “a” – a total spectrum, “b” – a spectrum of pulses with a short front, “c” – a spectrum of pulses with a long front.

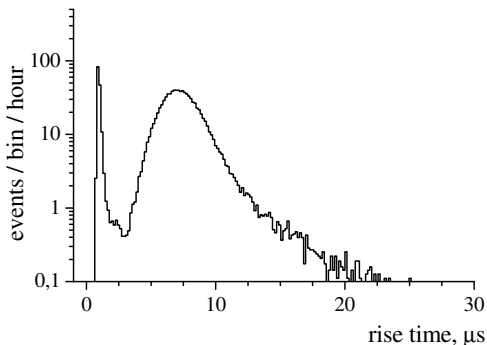


FIG. 4. Front duration distribution of pulses from the spectrum (a) from the Fig. 3 normalized for 1 hour.

The objects are placed in a list in an accordance of a thickness of the cosmic rays absorber above the installation in a sequence of 4900 m w.e. \rightarrow 0 m w.e. \rightarrow 1.3 m w.e. A brief description of the objects is given in [12].

A spectrum “a” was preliminary measured in the point (10) at 63.12 h to obtain a general imagine about statistical characteristics of pulses. The spectrum is shown on Fig. 3, spectrum (a). A distribution of the pulse front durations (0.2-0.8 region of the total amplitude normalized for 1 hour) is shown on the Fig. 4. The peaks in the regions of 0.5-1.6 μ s and 3.2-13 μ s are visible. The last one is correspond to the pulses from the scintillator. A selection of pulses correspondent to this marked regions allows one to separate the spectrum (a) on the Fig. 3 at fast [spectrum (b)] and slow [spectrum (c)] components. It is seen that the fast pulses contribute a main part at the low amplitudes. The more detailed analysis of the fast pulse shapes shows that the pulses have different decay shapes. Such difference could be explained by small variable contributions of the scintillation light to the PMT Cherenkov light. A proportion of the two components depends on a number of particles in an event and a quantity of tracks crossing the two light generators. A thin scintillator has a low sensitivity to the cosmic rays and electrons. Amplitudes of pulses of the events with

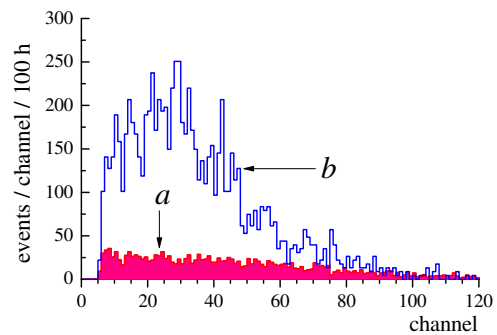


FIG. 5. The detector own background pulse amplitude spectrum “a” and the spectrum of a neutron calibration source “b”.

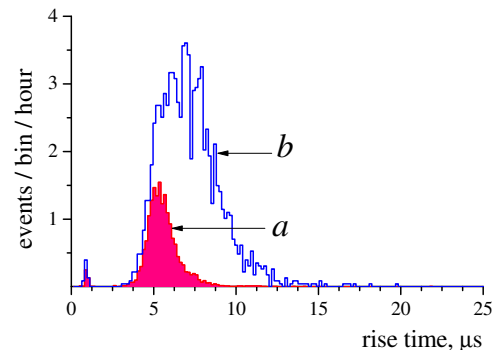


FIG. 6. Front duration distributions of pulses from the spectrum (a) (curve “a”) and spectrum (b) (curve “b”) from the Fig. 5 normalized for 1 hour.

the cosmic rays particles crossing of the scintillator are small and lie below the registration threshold.

Significant number of extraneous pulses could presence in the data sets measured with a low count rate in the underground conditions. Pickups from a periodic switching of industrial equipment and furnishings are the main component of such pulses. They have shapes differ considerably from the useful ones. The extraneous pulses could be excluded from the spectra by using of the discrimination on a base of a pulse shape analysis.

The detector own background should be known for the low count rate measurements. A measurement at the point (2) was done for this purpose. The spectrum normalized at 100 h is shown on the Fig. 5 [spectrum (a)]. The corresponding distribution of the front durations is shown on the Fig. 6 (curve “a”).

It is seen from a comparison of the spectra on the Fig. 5 that the background spectrum has a longer energy extension than the neutron one. Its front distribution is shifted to the shorter times simultaneously. A conclusion could be done that the detector background created by strongly ionized particles with the energy larger than the energy of the products of the neutron reactions. The α -particles from decays of the ^{232}Th and ^{238}U natural long lived radioactive isotopes and its daughters contained as micro impurities in the scintillator could be possible sources of

the background. The ^{210}Po ($T_{1/2} = 138.4$ d, $E_\alpha = 5.3$ MeV) generated in a decay chain of the ^{210}Pb (β^- - decay, $T_{1/2} = 21.8$ y) could be another background source. The last isotope was born charged in the air in the radon decay chain and deposited at the scintillator charged surfaces during its preparation. This source could be essentially suppressed by using of the special protecting arrangements against the radon and its daughters penetration into the gas environment of the scintillator production area. The α -particles which were born outside of the scintillator plate will be absorbed in the covering lavesan film and will not give any noticeable effect.

Estimated path lengths of α -particles with the energies of 2051 keV, 4800 keV and 5300 keV in the scintillator with a density of $3.0 \text{ g}\cdot\text{cm}^{-3}$ are equal to $10.6 \mu\text{m}$, $28.6 \mu\text{m}$ and $32.1 \mu\text{m}$ [8]. The one of the 2735 keV triton is $56.3 \mu\text{m}$. The energy spectrum extension will be longer due to the energy difference if the main source of the background is not the neutron reactions products but the α -particles from the ^{210}Po decays. A difference could increase additionally if a specific light yield of the ZnS(Ag) decreased at lower particle energy with an ionization density rise as it occurs for the other nonorganic scintillators [4]. The light output for the two reaction products with the 4800 keV sum energy will be less than the one for the α -particle with the same energy. The lesser front duration of the background pulses could be explained by a location of the α -source on a surface of the scintillator grains. Trajectories of α -particles will be directed into the grains in this case and the main part of energy will be released inside the ones. It is mentioned in the [4] that a scintillator based on the dispersed ZnS(Ag) has a long afterglow. It could be explained possibly by a relative increasing of long-lived excitation traps number located on grain surfaces. A particle absorbed in the grain surface layer will give a longer deexcitation time in this case. Vertexes of neutron reactions are distributed uniformly in a ^6LiF component volume. The reaction products should exit from this materials and fall into the surface layer of the ZnS(Ag) grain to produce a scintillation. An ionization density increases with a particle energy decreasing in accordance with the energy loss dependence [9]. A considerable part of the energy will be released in the surface layers of the two adjacent grains giving longer pulse front duration in comparison with a particle absorbed inside the grain. The features of the detector background distributions mentioned above could be an indirect evidence of a background source grains surface location.

Count rates of the detector at 1 hour for the data integrated above the third channel of the spectra “b” and “c” Fig. 3 are presented in the Table 1 for the all objects cited in the list.

Values of a thermal neutron flux F in the all examined points could be obtained from the neutron count rates. A flux F of particles according to a definition is a ratio of a particles number ΔN falling on a given surface at a Δt time interval to this interval: $F = \Delta N / \Delta t$. The

measured count rate \mathbf{n} connected with F by the $\mathbf{n} = \varepsilon \times F$ relation where ε is a neutron registration efficiency of the scintillation plate. A neutron flux density parameter ϕ is used usually to a lightening of a comparison of results obtained with the different geometry detectors. The ϕ according to a definition is a ratio of a particles flux dF_S penetrated into the volume of an elementary sphere to the area of it's central cross section dS : $\phi = dF_S / dS$. The dF_S value could be determined using a specific neutron flux falling on an elementary square of the scintillator as $dF_S = 4 \times F / S$ where S is an area of the scintillator plane and the coefficient 4 is equal to the ratio of the sphere surface area to the area of the sphere cross section. The ϕ is equal to $\phi = 4n / (2S\varepsilon)$ as a result.

It is seems impossible to calculate ε -value because of uncertainties of a composition and a structure of a scintillator layer. This value was obtained experimentally from a comparison of the n_1 count rate of the described detector and $n_{1(2)}$ count rate of the detector with an additional similar passive scintillator plate (2) put under the active plate (1). The plate (2) was light intercepted. The detector in the measurements was shielded by the 1 mm cadmium foil for the thermal neutron coming on from the upper hemisphere to shape a single-sided neutron flux. A count rate of the standard detector is equal to $n_1 = \varepsilon_1 \times F$ and the one for the modified detector is $n_{1(2)} = \varepsilon_{1(2)} \times (F - \varepsilon_2 \times F)$ where ε_1 is a plate (1) absorption efficiency of a thermal neutron flux F , $\varepsilon_{1(2)}$ is the absorption efficiency of thermal neutron flux plate (1) in the presence of isolation from the light of the plate (2) absorb some of the flux F with efficiency ε_2 . A value of efficiency is an integral characteristic of a process of absorption for the neutrons coming at different angles and depends on a path passed by a neutron in the scintillator. An angular distribution of neutrons after passing the one scintillator layer is pulled in the direction normal because of emptive absorption of particles coming at odd angles. An absorption will be lower for the passed neutrons and $\varepsilon_{1(2)}$ will be lower than ε_1 ($\varepsilon_{1(2)} \leq \varepsilon_1$). The count rates are specified by the expressions $n_2 = \varepsilon_2 \times F$ and $n_{2(1)} = \varepsilon_{2(1)} \times (F - \varepsilon_1 \times F)$ in a case when the plate (2) is used as the active one. Five unknown variables ε_1 , $\varepsilon_{1(2)}$, ε_2 , $\varepsilon_{2(1)}$ and F are in four obtained equations. One needs to measure additionally a total count rate $n_{[1+2]} = n_{[2+1]}$ for the case when the both plate used in the active mode to determine precisely all five values. Such measurement is possible if the plates emit scintillation light into the both hemispheres in the detector having two PMTs. The task could be solved with the reviewed detector if the plate adsorbs neutron not strongly. It could be taken that $\varepsilon_{1(2)} \approx \varepsilon_1$ and $\varepsilon_{2(1)} \approx \varepsilon_2$ in this case. Simple conversions give the expressions $\varepsilon_1 = [n_1 - n_{1(2)}] / n_2$ and $\varepsilon_2 = [n_1 - n_{1(2)}] / n_1$.

The measurements were done in the point (9) of the objects list. The result $\varepsilon_1 = \varepsilon_2 = 0.14 \pm 0.01_{\text{stat.}} \pm 0.02_{\text{sys.}}$ was obtained. A difference between ε_1 and $\varepsilon_{1(2)}$ is calculated for the two homogeneous plate having $\varepsilon = 0.14$ at a registration of isotropic neutron flux coming

TABLE I. Count rates of the detector at 1 hour for the data integrated above the third channel of the spectra (b) and (c) Fig. 3 and the thermal neutron flux densities.

No.	Place, conditions,	Count rate, hour ⁻¹ (3-256 channel)		Thermal neutron flux density, (s ⁻¹ ·cm ⁻²)
		Short pulse rise time	Long short pulse rise time	
1a	DULB-4900	0.13±0.03	21.3±0.4	(2.6±0.4)×10 ⁻⁵
1b	-//- + (Cd)	0.09±0.03	18.7±0.5	(1.2±0.4)×10 ⁻⁵
2	DULB-4900 (low background)	0.10±0.02	16.4±0.3	≤ 3.8 × 10 ⁻⁷ (90% C.L.) (³ He prop. counter)
3	-//- + (n-source)	0.2±0.1	80±2	(3.4±0.4)×10 ⁻⁴
4a	KAPRIZ	0.13±0.03	16.7±0.3	≤ 5.9 × 10 ⁻⁶ (90% C.L.)
4b	-//- + (Cd)	0.13±0.03	16.5±0.4	≤ 5.9 × 10 ⁻⁶ (90% C.L.)
5a	NIKA	0.19±0.04	17.8±0.4	(7.5±3.1)×10 ⁻⁶
5b	-//- + (Cd)	0.14±0.03	16.9±0.3	(3.4±3.1)×10 ⁻⁶
6a	μ-detector	8.4±0.5	64±1	(2.8±0.3)×10 ⁻⁴
6b	-//- + (Cd)	8.2±0.4	43±1	(1.4±0.2)×10 ⁻⁴
7a	ELLING	23±1	1415±8	(7.5±0.6)×10 ⁻³
7b	-//- + (Cd)	22±3	730±16	(3.8±0.4)×10 ⁻³
8a	Open soil	28±3	1704±31	(9.0±0.8)×10 ⁻³
8b	-//- + (Cd)	27±3	702±14	(3.7±0.3)×10 ⁻³
9	LAB, 404	22±1	1439±9	(7.6±0.6)×10 ⁻³
10a	LAB, 204	16±2	866±14	(4.5±0.4)×10 ⁻³
10b	-//- + (Cd)	16±1	482±6	(2.5±0.2)×10 ⁻³
11	LAB, 211	19.1±0.9	672±5	(3.5±0.3)×10 ⁻³
12	LAB, ground	6.5±0.5	240±3	(1.2±0.1)×10 ⁻³

from the one side uses as a systematic uncertainty.

A background count rate measured in the point (2) was subtracted from the data in a process of a determination of a thermal neutron flux density in the each other point. The obtained ϕ -values are resulted in the last column of the Table I. A limit of a thermal neutron flux density in the point (2) was obtained on a base of measurements with a CH-04 neutron proportional counter with ³He [14].

Discussion of results

A specific own background of the scintillator plate was found to be to $(2.69±0.05) \text{ h}^{-1} \times (100 \text{ cm})^{-2}$ in the point (2). This value is comparable with a value of a surface α -activity of the commercial copper and steel samples which is $\sim (0.5 - 1.0) \text{ h}^{-1} \times (100 \text{ cm})^{-2}$ [10]. A surface α -activity of the silicon semiconductor samples could reach $\sim 0.1 \text{ h}^{-1} \times (100 \text{ cm})^{-2}$. It is seems possible to prepare a scintillator plate with similar surface α -activity by using of a specially selected low background [ZnS(Ag)+⁶LiF] material and a clean technology for the plate preparation. A sensitivity of such scintillator detector (SD) for the thermal neutrons would be comparable with a sensitivity of the ³He-proportional counter. A present ratio of the sensitivities is ~ 16 as it is seen from a comparison of the data for the (2) and (4) points of the Table I. A difference of the front time duration distribution of

background and neutron pulses could be useful for the plate sensitivity improving also. The obtained results are in a good agreement with the one measured by the ³He-proportional counter in the Ref. [11].

A value of the own background defines a sensitivity of the neutron measurement in the deep underground conditions as it seen from the Table I. A count rate of neutrons in the DULB-4900 (point (1a)) is equal to $(21.32-16.4)/6.11=(0.8±0.08) \text{ h}^{-1} \times (100 \text{ cm})^{-2}$ with the effect to background ratio equal to ~ 0.3 . The neutrons are born in the rock mainly due to the (α, n) -reactions with the light elements. Walls of the “KAPRIZ” laboratory are covered with a 30 cm layer of a low background concrete made on a base of a dunite crushed rock. The concrete is decreased considerably a neutron flux from the rock. (The dunite concrete was used in the construction of the “NIKA” laboratory too). A comparison of neutron fluxes in the “DULB-4900” and “KAPRIZ” measured with CH-04 proportional counter shows that the concrete decreases a neutron flux at ~ 5.2 times. One can estimate an expected neutron effect in the “KAPRIZ” using of this coefficient and SD count rate in the point (1a) as $(0.15±0.02) \text{ h}^{-1} \times (100 \text{ cm})^{-2}$. A calculation with the data from the Table I gives a value $(0.05±0.08) \text{ h}^{-1} \times (100 \text{ cm})^{-2}$ which is not contradicts to the estimated one. The last value was used to obtain a limit for the neu-

tron flux density in the points (1a and 1b) at 90% C.L. as $2 \times (0.05 + 1.64 \times 0.08)/3600/100/0.17 = 5.9 \times 10^{-6} \text{ cm}^{-2}\text{c}^{-1}$.

The own SD background enters a minor deposit into the detector count rate in the measurements at the ground and shallow underground points where reactions of cosmic rays with element nuclei of the environment are the main source of the neutron.

A comparison of the SD count rates with and without a cadmium absorber shows that the absorber decreased a neutron flux at ~ 1.9 times under a ceiling and at ~ 2.4 times on the open place. Thus, a ratio of neutron fluxes from the soil and from the atmosphere on the open place is equal to ~ 1.4 .

A SD count rate of the short front pulses in the underground conditions does not depend practically on a value of the external γ -quanta background level as it seen from the Table I. This noise component could be born directly in the PMT by densely ionizing particles. The pulses could appear at the photocathode as a result of direct generation of electrons by α -particles of the window surface α -activity. A count rate of such pulses connected with the muon intensity and increased proportionally with its growth.

Conclusions

Measurements of some working characteristics of a thermal neutron scintillator detector prepared on a base of a thin $216 \times 304 \text{ mm}^2$ plate of a fine-grained $[\text{ZnS}(\text{Ag}) + {}^6\text{LiF}]$ - scintillator made at the BNO INR

RAS. An analysis of shapes of charge pulses recorded by means of a digital oscilloscope has showed that background pulses with a short front created by the cosmic rays directly in the photomultiplier are presented among the working pulses in a low energy region of spectra. Measurements of the detector thermal neutron count rate were made at the ground and underground objects of the BNO INR RAS at different shielding for the cosmic rays. The inherent background of the detector created by α -particles from decays of inner radioactive admixture with a surface α -activity at level of $(2.69 \pm 0.05) \text{ h}^{-1} \times (100 \text{ cm}^{-2})^{-1}$ was measured. A ratio of an effect to a background was equal to ~ 0.3 at the underground conditions. The neutron pulses have a shorter front than the background ones. It could be used for a discrimination of the background pulses at ~ 2 times with an insignificant rejection of the neutron events at the low neutron flux measurements.

Acknowledgement

The work was carried out in part with the financial support of the Federal Objective Program of the Ministry of Education and Science of the Russian Federation "Research and Development in the 2007-2013 years on the Priority Directions of the Scientific and Technological Complex of the Russia" under the contract No. 16.518.11.7072 and the "Russian Foundation for Basic Research" under the grant No. 14-22-03059.

We are thankful to Yu.V. Stenkin for providing the samples of the scintillator and numerous useful critical comments.

-
- [1] V.V. Alekseenko, Yu.M. Gavriluk, D.M. Gromushkin, et al., "Correlation of Variations in the Thermal Neutron Flux from the Earth's Crust with the Moons Phases and with Seismic Activity" // *Physics of the Solid Earth*, 2009, Vol. 45, No. 8, p.709.
- [2] V.V. Alekseenko, D.D. Dzhappuev, V.A. Kozyarivsky, et al., "Analysis of Variations in the Thermal Neutron Flux at an Altitude of 1700 m above Sea Level" // *Bulletin of the Russian Academy of Sciences: Physics*. 2007, Vol. 71, No. 7, p. 1047
- [3] A.I. Abramov, Yu.A. Kazansky and E.S. Matusevich, *Bases of the Experimental Methods of Nuclear Physics*, Moscow: Energoatomizdat, 1985.
- [4] M.N. Medvedev, *Scintillation detectors*. Moscow: Atomizdat 1977.
- [5] Phosphor data - www.appscintech.com. ${}^6\text{LiF}/\text{ZnS}:\text{Ag}$ Phosphor/Scintillator Data Sheet 39- ND - iss1.doc.
- [6] "PHOTOMULTIPLIER TUBES (principles and applications)". Produced and distributed by Philips Photonics International Marketing. BP 520, F-19106 BRIVE, France. Philips Export B.V. 1994.
- [7] M.E. Globus, B.V. Grinev, *Inorganic scintillators (new and traditional materials)*. Kharkiv: Akta, 2001.
- [8] O.F. Nemets, Yu.V. Ghofman, *Handbook of Nuclear Physics*. Kiev: Naukova Dumka. 1975.
- [9] M.J. Berger, J.S. Coursey, M.A. Zucker and J. Chang, *Stopping-Power and Range Tables for Electrons, Protons, and Helium Ions*. NIST, Physical Measurement Laboratory, <http://www.nist.gov/pml/data/star/>
- [10] E.L. Kovalchuk, V.V. Kuzminov, A.A. Pomansky, "Surface alfa activity of different materials". *Proc. of the Int. Conf. "The Natural Radiation Environment III"*, Houston, Texas, April 23-28, 1978, V.1, 1980, P.673.
- [11] V.V. Alekseenko, I.R.Barabanov, R.A. Etezov, et al., "Results of measurements of an environment neutron background at BNO INR RAS objects with the helium proportional counter" // arXiv: 1510.05109 [physics.ins-det].
- [12] V.V. Kuzminov., "The Baksan Neutrino Observatory". // *Eur. Phys. J. Plus* 127 (2012) 113. doi: 10.1140/epjp/i2012-12113-0; <http://www.inr.ac.ru/>
- [13] V.P. Mashkovich, A.V. Kudryavtseva, *Handbook "Protection from ionizing radiation"*. Moscow, Energoatomizdat, 1995.
- [14] A.Kh. Khokonov, Yu.V. Savoiskii, A.V. Kamarzaev, "Neutron Sensitivity and Detection Efficiency of ${}^3\text{He}$ - and ${}^{10}\text{F}_3$ -Counters" // *Physics of Atomic Nuclei*, V.73, No.9, 2010, P.1482.